Advances in Concrete Construction, *Vol. 9, No. 5 (2020) 437-448*
DOI: https://doi.org/10.12989/acc.2020.9.5.437

Influence of connection detailing on the performance of wall-to-wall vertical connections under cyclic loading

S. Hemamalini[a] and R. Vidjeapriya*

College of Engineering, Guindy, Anna University, Chennai, India

(*Received November 8, 2019, Revised March 14, 2020, Accepted March 25, 2020*)

Abstract. In high rise buildings that utilize precast large panel system for construction, the shear wall provides strength and stiffness during earthquakes. The performance of a wall panel system depends mainly on the type of connection used to transfer the forces from one wall element to another wall element. This paper presents an experimental investigation on different types of construction detailing of the precast wall to wall vertical connections under reverse cyclic loading. One of the commonly used connections in India to connect wall to wall panel is the loop bar connection. Hence for this study, three types of wet connections and one type of dry connection namely: Staggered loop bar connection, Equally spaced loop bar connection, U-Hook connection, and Channel connection respectively were used to connect the precast walls. One third scale model of the wall was used for this study. The main objective of the experimental work is to evaluate the performance of the wall to wall connections in terms of hysteretic behaviour, ultimate load carrying capacity, energy dissipation capacity, stiffness degradation, ductility, viscous damping ratio, and crack pattern. All the connections exhibited similar load carrying capacity. The U-Hook connection exhibited higher ductility and energy dissipation when compared to the other three connections.

Keywords: precast concrete; wall to wall; wet connections; dry connections; reverse cyclic loading

1. Introduction

A shear wall is one of the structural elements used in high rise buildings to resist the wind and seismic loads due to high initial stiffness and lateral load resisting ability (Soudki *et al*. 1996). In the precast large wall panel system, the connections play an important role in the transfer of different types of loads from one structural member to another structural member. During past earthquakes, many large panel systems suffered a lot of damage. Some of the typical damages observed in large panel systems during the Christchurch earthquake, 2011, was the failure of steel connectors and diagonal bracings, cracking of inter-panel connections, and several complete collapses of the wall panels. Failure of the wall was observed in-plane along the base followed by the loss of anchorage. In under construction buildings, connections between the orthogonal panels had failed, leading to a out-of-plane collapse of one panel and destabilisation of the other (Kam *et al*. 2011). The behaviour of wall panels during past earthquakes indicates that the connection forms the weakest link in the structure. The connections should exhibit good ductility and energy dissipation capacity to resist seismic loads.

2. Connections

Precast members are connected by two methods, the first one being the “Equivalent monolithic system”. Park (2003) described that the connection is achieved by protruding longitudinal bars that are connected either by lap splices in a cast-in-place concrete joint, by non-contact lap splices involving grouted steel corrugated ducts, by splice sleeves, by welding, by mechanical connectors, or using grouted post-tensioned tendons. Precast walls with a vertical connection using loop bars in cast-in-situ concrete were studied by many researchers (Rossley *et al.* 2014a, Sorensen *et al*. 2015, Vaghei *et al*. 2016, Biswal *et al*. 2018, Vaghei *et al*. 2019). The observations made were that an increase in the ratio of transverse reinforcement and overlapping length of loop bars showed an increase in the ductility of the connections. Reinforced concrete members with loop joints exhibited similar ultimate behaviour, ductility and strength to ordinary RC members without joints under static and fatigue loading (Ryu *et al*. 2007).

The second one is the “Jointed construction” where the structural members are connected by dry connections formed by welding or bolting reinforced bars, plates or stud embedment’s and dry packing and grouting (Park 2003). Many studies were conducted on dry connections using dowel bars as the connecting element (Smith 2016, Pramodh *et al*. 2018, Sorensen *et al.* 2017a). It was observed that dowel bars embedded in corrugated steel ducts created a higher confinement effect, allowing for a reduction in required embedment length (Smith 2016, Pramodh *et al*. 2018). The specimens with a relatively lower compressive strength at the interface had a greater displacement capacity and a higher ultimate load than specimens with a relatively higher compressive strength (Sorensen *et al.* 2017a). Precast walls with horizontal

*Corresponding author, Ph.D.
E-mail: vidjeapriya@annauniv.edu
[a]Ph.D. Student
E-mail: samkanhema@gmail.com

ISSN: 2287-5301 (Print), 2287-531X (Online)

connections using unbonded PT steel has been studied by many researchers (Holden *et al.* 2003, Perez *et al.* 2007, Perez *et al*. 2013, Erkmen and Schultz 2009, Henry *et al*. 2012, Belleri *et al*. 2014). The unbonded PT connections exhibited low energy-dissipation capacity, hence further research was carried out by providing supplementary energy dissipation components (Ajrab *et al*. 2004, Kurama 2005, Restrepo and Rahman 2007, Marriott *et al*. 2008, Smith and Kurama 2014, Smith *et al*. 2011, Smith *et al*. 2013, Smith *et al*. 2015). Precast walls connected by welded plate connectors showed increased shear resistance with less ductility (Hofheins *et al*. 2002).

3. Previous studies on the vertical wall to wall connection

The connection between wall to wall panels can either be in a vertical or horizontal direction. One of the commonly used connections in India to connect precast walls in the vertical direction is the loop bar connection. The behaviour of the loop bar connection between wall to wall panels was studied under monotonic loading (Vaghei *et al*. 2016, Biswal *et al*. 2018, Rossley *et al.* 2014b). Loop bar connections were used to transfer the load from one precast element to another precast element. It was observed that the load carrying capacity of the specimen was high when the spacing between the loop bar was less because of the generation of strut and tie action and increased dowel action under monotonic loading. Under shear loading, the connection exhibited ductile behaviour before failure.

The ultimate load carrying capacity of the loop bar connection in tension was improved by increasing the overlapping length of U-bar, decreasing the spacing between adjacent U-bars, increasing the amount of transverse reinforcement, and increases the cross-sectional diameter of the U-bar (Ong *et al*. 2006, Joergensen and Hoang 2013, Araujo *et al.* 2014). Li and Jiang (2016) concluded that smaller spacing of reinforcement with a higher amount of reinforcement showed greater load resistance with less ductility under shear loading. The width of the joint was influenced by the diameter of the loop bar used in the connection (Ryu *et al*. 2007). Joergensen and Hoang (2013) investigated experimentally and concluded that the failure of the connection depended on the yielding strength of the loop bar and joint concrete strength. An experimental study was conducted on wall panels connected by channel section. The capacity of the channel connection was greater than the loop bar connection under rotational loading (Taheri *et al*. 2016). Under lateral load, the channel section exhibited better flexural strength and energy dissipation capacity, when compared to the loop connection (Vaghei *et al*. 2019). Cracks were evenly distributed due to cyclic load and exhibited a ductile failure mode (Vaghei *et al.* 2017). Precast wall panels with shear keys exhibited higher shear resisting capacity under tensile loading (Sorensen *et al*. 2017b, Sorensen *et al*. 2018), monotonic loading (Ibrahim *et al.* 2014), and lateral loading (Sorensen *et al.* 2015). Under Quasi-static cyclic loading, lateral load resistance and stiffness of the vertical connection was increased by adding strength and more steel shear keys at

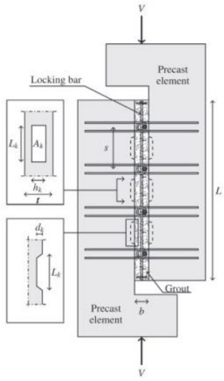

Fig. 1 General geometry of wall to wall vertical connection with shear keys (Sorensen *et al*. 2018)

the connection (Shen *et al.* 2019). Precast shear walls using U-bar loops (vertical plane) reinforced with double T-headed bars with shear keys showed a ductile response when compared to conventional U-bar loops (horizontal plane) (Sorensen *et al*. 2016). The shear capacity of a vertical shear connection using wire loops was prone to be governed by the failure of the joint mortar in combination with yielding of the locking bar (Joergensen *et al.* 2015). Vertical shear connections using wire loops failed by the development of yield lines (failure mode 1) only along the joint surfaces, when the mechanical degree of wire loops was low and by development of diagonal yield lines (failure mode 2) running across the connection, when the mechanical degree of wire loops is high (Joergensen *et al.* 2017). Fig. 1 shows General geometry of wall to wall vertical connection with shear keys.

4. Significance of this study

Precast construction technology may replace the conventional methods to reduce the duration of construction and also to improve the quality of construction. Due to the increase in population in India, people started moving to high rise buildings. To increase the stability of the structure for high rise buildings, the shear wall panel system was introduced. In the precast wall panel system, the connections play a vital role in transferring the forces from one panel to another panel, especially during earthquakes. Hence, there is a need to develop a strong and stable connection between the wall to wall panels. In the present work, the behaviour of a precast shear wall to wall vertical connection using three wet and one dry connections i) Wall to Wall Staggered Loop bar precast connection (WW-SL), ii) Wall to Wall Equally spaced Loop bar precast connection (WW-EL), iii) Wall to Wall U-Hook precast connection (WW-UH), iv) Wall to Wall Channel connection (WW-CH) was studied. The objective of the present study was to investigate the influence of the connection detailing on the cyclic behaviour of the precast wall to wall vertical connection.

5. Design and detailing

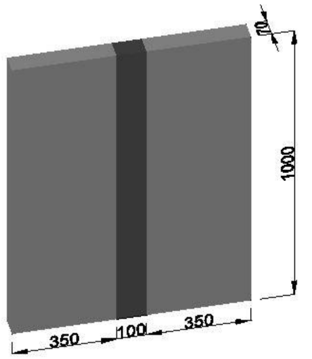

Fig. 2 Schematic diagram of the precast wall to wall connection

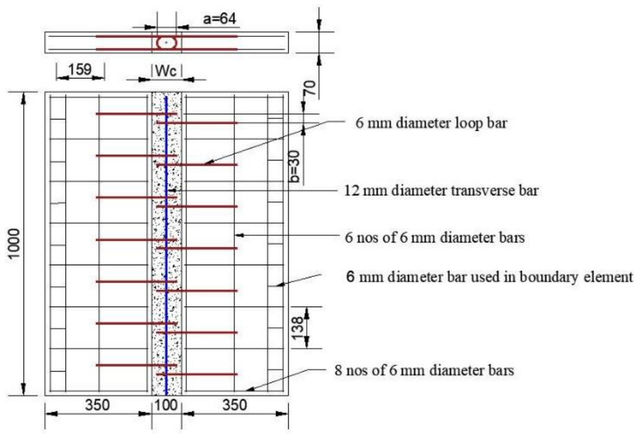

Fig. 3(a) Reinforcement detailing of (WW-SL) connection

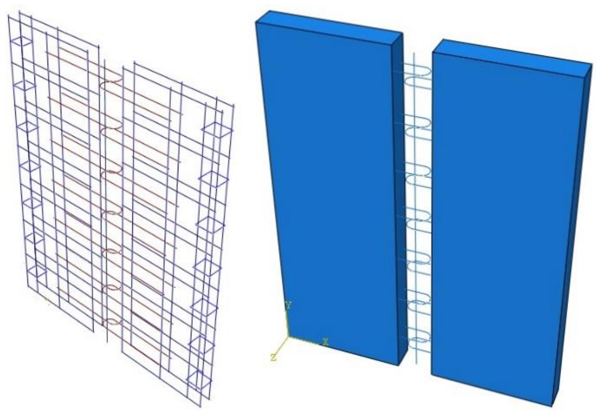

Fig. 3(b) 3D view of (WW-SL) connection

The critical wall panel was designed according to IS456:2000 and IS 13920:2016. The experimental program describes the cyclic shear behaviour of the vertical connection between the precast wall panels using different connections for a scaled model using a scale factor of 1:3. Four specimens were cast for the experimental work. Each specimen consists of two wall panels with a connection at the centre. Each wall panel size was 350×1000 mm and the width of connection was 100 mm. Thickness of the wall was 70 mm. Fig. 2 shows the schematic diagram of the precast wall to wall connection.

6. Material properties

A concrete mix, designed for a characteristic cube compressive strength of 30 N/mm^2 as per the Indian code of practice (IS 10262-2009) was used to cast the wall panels and the connections. The compressive strength of concrete was determined by casting 150×150×150 mm concrete cubes. The 28th day compressive strength for the wall panels and the connections was 39.52 N/mm^2 and 41.97 N/mm^2 respectively. The deformed bars (Fe415) was used in the design of the wall panels and the connection reinforcement.

7. Types of wall to wall connections

7.1 Staggered loop connection (WW-SL)

Two walls were connected using loop bars (180 bent up bars). It was projected from both the walls and overlapped in the connection region. The transverse bar was inserted between the overlapping loop region to withstand the tensile forces caused due to the inclined stress field developed between the overlapping loops. It also provides confinement to the concrete in the overlapping area. The spacing between adjacent overlapping loops is usually about 2-6 times the diameter of the bar to account for construction tolerances (Joergensen and Hoang 2013). For this connection spacing between the overlapping loops was taken as 5ϕ. The spacing between the overlapping loop reinforcement was 30 mm whereas the spacing between the main reinforcement and loop was 45 mm. Development length, anchoring length, and details of loop connection were calculated according to IS 456:2000. Anchoring length of the loop bar was measured from the end of the wall to outside end of bent. The development length of the bar was measured as the length of the loop anchored inside the wall panel. The reinforcement details and a 3D view of the (WW-SL) connection respectively, are shown in Figs. 3(a)-(b).

7.2 Equally spaced loop connection (WW-EL)

The detailing of the loop reinforcement was the same as that of the staggered loop connection (WW-SL). The spacing between the overlapping loops was taken as 6.7ϕ. This spacing was adopted to observe the behaviour of the overlapping loop connection if spacing exceeded the range of as suggested by Joergensen and Hoang (2013). The spacing between overlapping loops was same throughout the height of the wall. The spacing between the loop reinforcement was 40mm. The spacing between main wall reinforcement and loop was also maintained as 40 mm. Figs. 4(a)-(b) show the reinforcement details of the (WW-EL) connection and a 3D view of the (WW-EL) connection, respectively.

7.3 U-Hook connection (WW-UH)

Two U-shaped reinforced bars were used in each

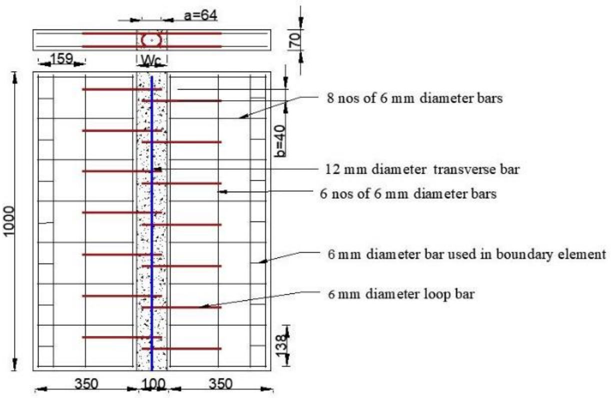

Fig. 4(a) Reinforcement detailing of (WW-EL) connection

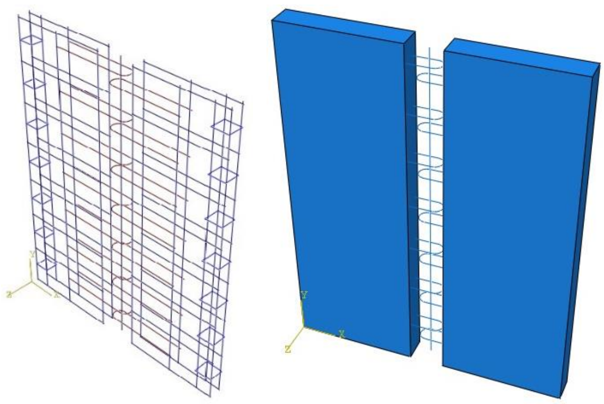

Fig. 4(b) 3D view of (WW-EL) connection

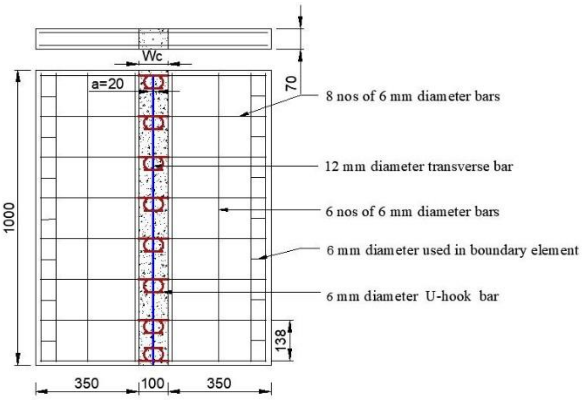

Fig. 5(a) Reinforcement detailing of (WW-UH) connection

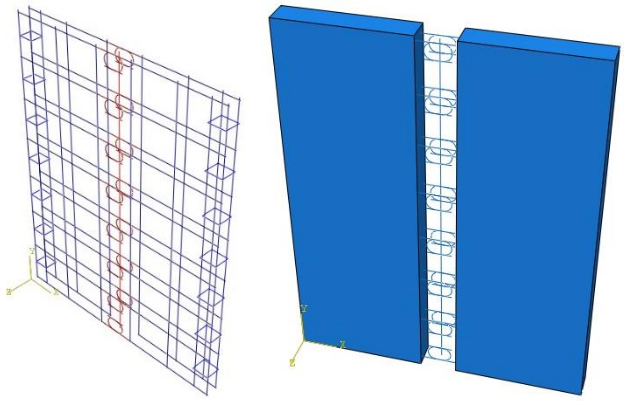

Fig. 5(b) 3D view of (WW-UH) connection

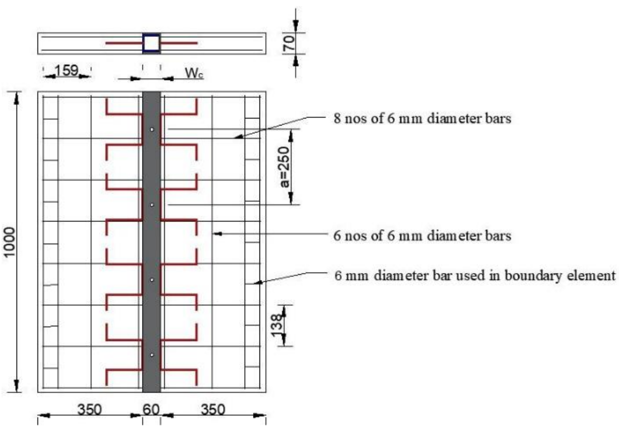

Fig. 6(a) Reinforcement detailing of channel connection (WW-CH)

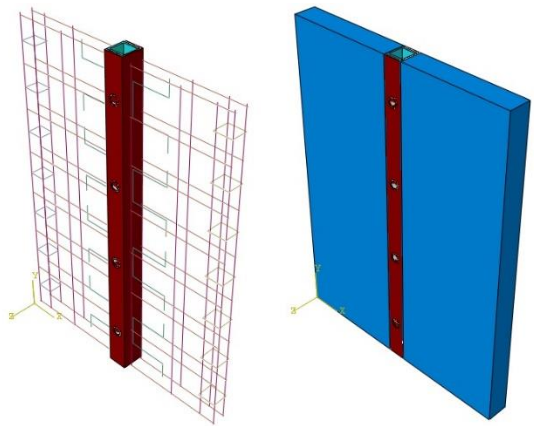

Fig. 6(b) 3D view of (WW-CH) connection

overlapping area to connect the two walls. It was an extension of the horizontal reinforcement from both walls and overlapped in the connection region. The transverse bar was inserted in the connection region. The transverse bar is provided to give confinement to the concrete in the connection region and to prevent propagation of the cracks. It does not play any role in the transfer of the tensile forces between the wall elements. Figs. 5(a)-(b) show the reinforcement detailing of the (WW-UH) connection and a 3D view of the (WW-UH) connection, respectively. The development and anchorage lengths provided was according to IS 456:2000.

7.4 Channel connection (WW-CH)

The right-side wall panel and left side wall panel was connected by a dry connection using two channel sections. The channel sections were designed according to IS 800: 2007 subjected to combined shear and bending. Reinforcement details and a 3D view of the (WW-CH) connection, respectively are as shown in Figs. 6(a)-(b). The thickness of the channel section was 6 mm. The channel section on the left-hand side was smaller than that on the right-hand side (both channel sections were fitted in such a manner that it formed a box-like cross section with one section fitted inside the other channel). Fig. 7 shows the

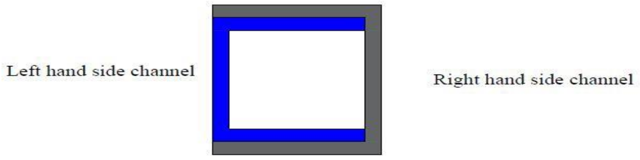

Fig. 7 Box like *c/s* formed by channel section

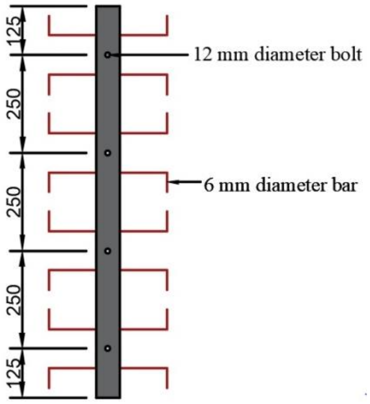

Fig. 8 Connection details of (WW-CH) connection

Table 1 Dimension details of connections

Specimen designation	W_c (mm)	A_{st} (mm^2)	a (mm)	b (mm)
Staggered loop bar connection (WW-SL)	100	791.68	64	30
Equally spaced loop bar connection (WW-EL)	100	791.68	64	40
U-Hook connection (WW-UH)	100	904.77	20	44
Channel connection (WW-CH)	60	452.38	250	-

Note: A_{st}=Area of reinforcement across the connection
W_c=Width of the connection
a=Overlapping length
b=Spacing between overlapping loops

cross section of the channel section. Both the channel sections were bolted together by using 12 mm bolts. For providing good bonding between the channel sections and wall panels, each channel section was tied to the wall panel using four hooks. With respect to buildability, this type of connection is very easy to construct as it is a bolted connection. The left and right wall panels are cast with the channel section, then it is assembled at the site. Fig. 8 shows the reinforcement details and a 3D view of the (WW-CH) connection, respectively. Table 1 shows the details of all the precast connections.

8. Construction of specimens

The specimens were constructed in two stages. In the first stage, two precast wall panels were cast. After the walls achieved 7th days strength, the joint face of both walls was prepared for bonding with new concrete by applying Nito-bond EB base. In the second stage, the connection region was concreted and then cured for 28days to achieve strength. All the connections, except the channel connection were wet connections.

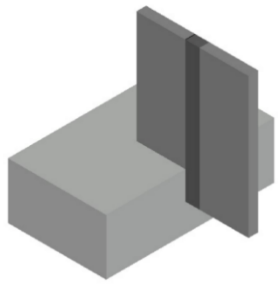

Fig. 9 Wall to wall connection with foundation block

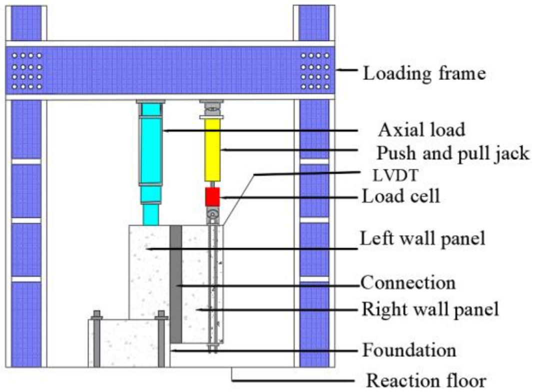

Fig. 10 Schematic diagram of loading test setup

9. Test setup

The cyclic load was applied at the top of the right panel with a displacement control method by using a push and pull jack. The jack had a push capacity of 25T and pull capacity of 15T and it was fixed to a loading frame with a capacity of 100 T. A load cell was used to measure the load. An axial load equal to $0.1f_c'A_g$ (Cheok and Lew 1993) was applied at the top of the left panel as uniformly distributed load and it simulated the gravity load on the wall panel. The left wall panel bottom was connected to the foundation block. The connection and the right wall panel were projected outside the foundation block like a cantilever. The foundation block of the test specimen was connected to the testing floor using four anchor bolts. Fig. 9 shows the wall to wall connection with the foundation block. Linear Variable Differential Transducer (LVDT) were used to measure the vertical displacement of the wall. The LVDT was connected at top of the Right panel. A schematic diagram of the test setup is shown in Fig. 10 and a Photograph of the test setup is shown in Fig. 11.

10. Cyclic loading

Every structure has a strength and stiffness to resist external load. The displacement control method was used to evaluate the performance of the structure. The sequence of cyclic loading adopted was similar to that adopted by Vidjeapriya and Jaya (2013). Three cycles were applied for each displacement level. The displacement cycle starts with 1 mm displacement, and ended with 28 mm displacement. Fig. 12 shows the sequence of cyclic loading. Drift ratio is

Fig. 11 Photograph of the test setup

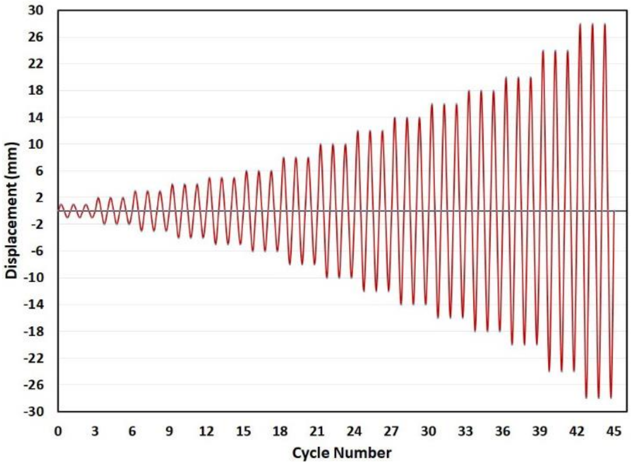

Fig. 12 Cyclic loading history

defined as the ratio of lateral displacement of the wall to the length of the wall (Yu *et al*. 2019).

11. Discussion of results

11.1 Strength

The ultimate load carrying capacity of the various connections such as the Staggered Loop bar connection (WW-SL), the Equally spaced Loop bar connection (WW-EL), the U-Hook connection (WW-UH) and the Channel connection (WW-CH) were 37 KN, 38 KN, 34 KN and 38 KN respectively, in the positive direction (upward) as shown in Fig. 13. The load carrying capacity of specimens (WW-SL) and (WW-EL) was nearly same. This may be due to the presence of the same area of reinforcement in the connection region. As shown in Fig. 13 the ultimate load carrying capacity of the channel section (WW-CH) is same as that of connection (WW-EL). But it is to be noted that the percentage of reinforcement in the connection region of the channel connection (WW-CH) is approximately 43% of that of connection (WW-EL) and (WW-SL). This may be due to the presence of a bolted connection between the two channel sections inserted in the wall panels. This type of interlinking is not present in any other connection. Hence, with lesser reinforcement higher load carrying capacity

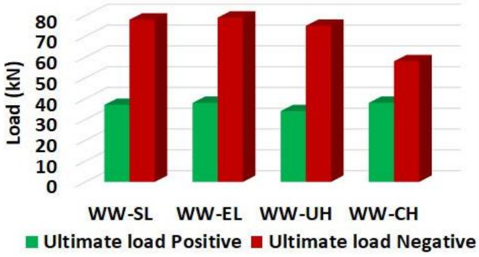

Fig. 13 Ultimate load of all the connections

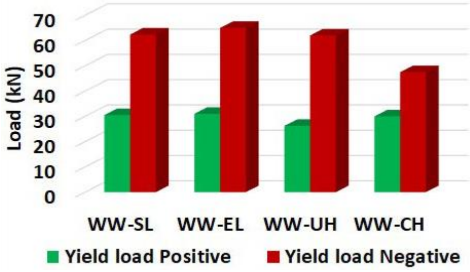

Fig. 14 Yield load of all the connections

Table 2 Ultimate load and yield load of all the connections

Connection Type	Yield load		Ultimate load		Ratio of Ultimate load to yield load		Average
	Positive	Negative	Positive	Negative	Positive	Negative	
WW-SL	30.5	62.37	37	78	1.21	1.25	1.23
WW-EL	31	65	38	79	1.23	1.22	1.22
WW-UH	26.25	62	34	75	1.30	1.21	1.25
WW-CH	30	47.5	38	58	1.27	1.22	1.24

could be achieved.

The load carrying capacity of the specimen (WW-UH) was 10% and 8% lesser than specimens (WW-EL) and (WW -SL) respectively, due to concrete spalling at -18 mm displacement cycle and reinforcement were exposed in the connection region near the foundation block. The transverse reinforcement inserted in the connection region was not effective for the connection (WW-UH). The maximum load was attained at 8mm displacement cycle for specimens (WW-SL), (WW-EL), and (WW-CH), whereas for (WW-UH) the maximum capacity was attained at 20 mm displacement cycle in the positive direction (upward).

The ultimate load in the negative direction (downward) was higher than that in the positive direction (upward) because the unsupported wall panel was bearing into the foundation block in the downward direction of loading. The channel section exhibited lesser load carrying capacity in the negative direction when compared to all other connections. This could be due to the debonding of concrete at the interface of the channel section in the top region. Fig. 14 shows the yield load of all the connections. The ratio of the maximum ultimate load to yield load was nearly the same for all types of connections. This indicates that the safety assurance of all the connections was the same as shown in Table 2.

11.2 Hysteretic behaviour

A hysteresis curve indicates the elastic (reversible) and

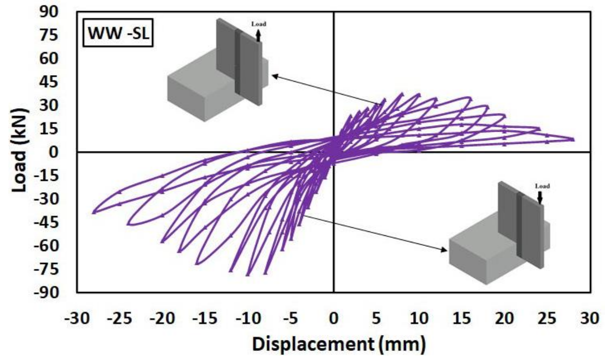

Fig. 15 Hysteresis curve of (WW-SL)

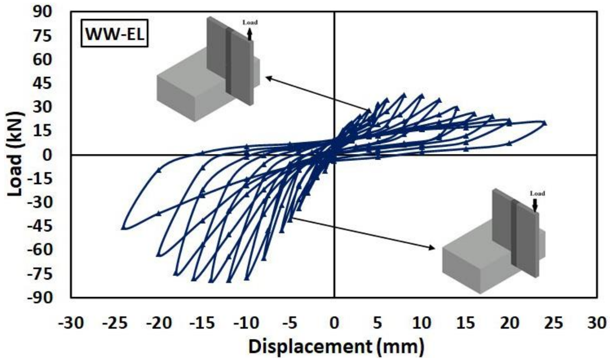

Fig. 16 Hysteresis curve of (WW-EL)

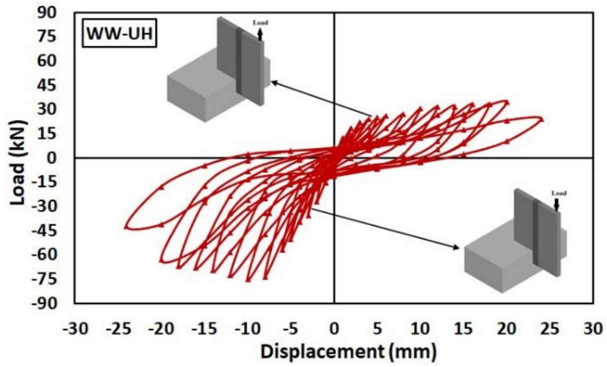

Fig. 17 Hysteresis curve of (WW-UH)

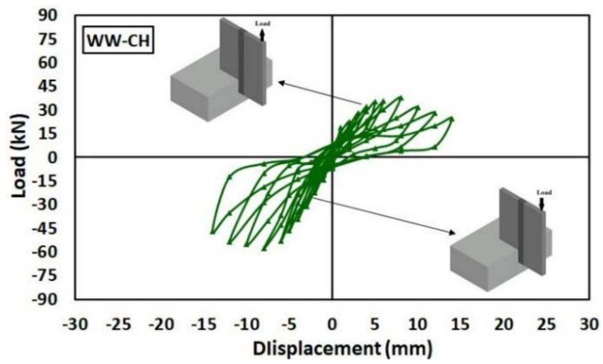

Fig. 18 Hysteresis curve of (WW-CH)

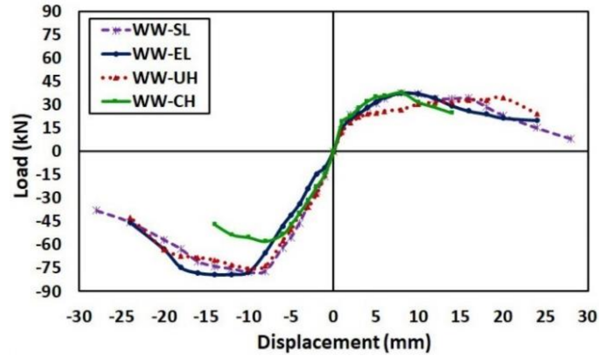

Fig. 19 Load-displacement envelopes of all the connections

plastic (irreversible) deformation of a structure during loading and unloading conditions in both positive and negative direction. Figs. 15-18 show the hysteresis curves of the specimens (WW-SL), (WW-EL), (WW-UH), and (WW-CH), respectively. For all the specimens, except for specimen (WW-CH), the hysteresis curves were wide and stable. This is an indication of good energy dissipation. Initially, up to a 5 mm displacement cycle, the hysteretic curve was formed without any pinching. After the 5 mm displacement cycle, the hysteretic loop exhibited a pinching effect.

11.3 Load-displacement envelope curve

The strength and stiffness of the connections increased initially due to a hardening behaviour, then after yielding occurred the strength and stiffness of the connection reduced due to a softening behaviour. Load-displacement envelopes of all the connections are shown in Fig. 19. For specimens (WW-SL), (WW-EL), and (WW-UH), the load carrying capacities increased gradually after the initiation of cracking. This was due to the tensile capacity of the loop bars. After the ultimate load was reached, there was a gradual decrease in the load carrying capacity and it was an indication of a ductile behaviour of the connection. In the case of the (WW-CH) connection, after ultimate load there was a sudden drop in the load carrying capacity due to a sudden loss of bond between the channel section and the wall panel in the top region.

11.4 Load ratio:

The Load ratio was used to examine the load carrying capacity of different connections from the yield load to failure load. The Load ratio is the ratio of the maximum load carrying capacity of each cycle to the yield load (Alameddine and Ehsani 1991) of the corresponding specimen. The yield load was calculated according to Park (1988). Fig. 20 shows the load ratio of all the connections. Load ratio increased linearly up to the ultimate load for all the connections. The load carrying capacity of the specimens (WW-SL), (WW-EL), and (WW-UH) was maintained throughout the displacement cycle, because of the confinement provided by the reinforcement in the connection region. The load carrying capacity was maintained beyond the yield point up to 16mm, 18mm, and 20mm displacement cycles for specimens (WW-SL), (WW-EL), and (WW-UH), respectively. In the connection (WW-CH) there was a sudden drop in the load carrying capacity after 8 mm.

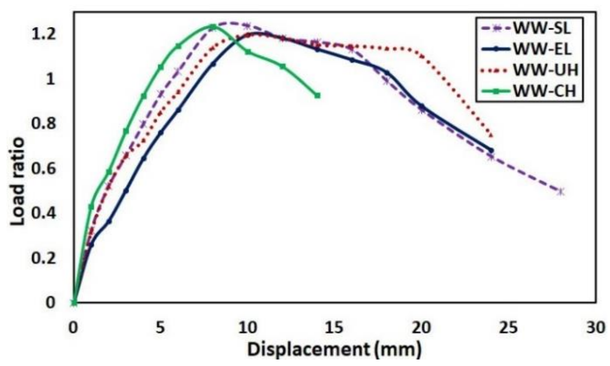

Fig. 20 Load ratio of all the connections

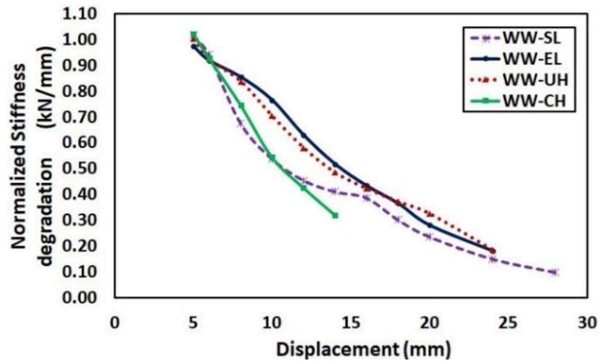

Fig. 22 Normalized Stiffness degradation of all the connections

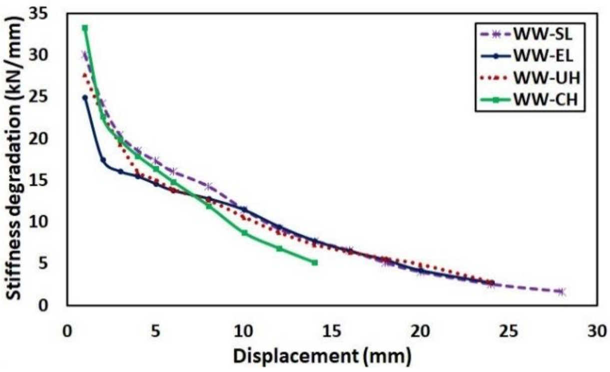

Fig. 21 Stiffness degradation of all the connections

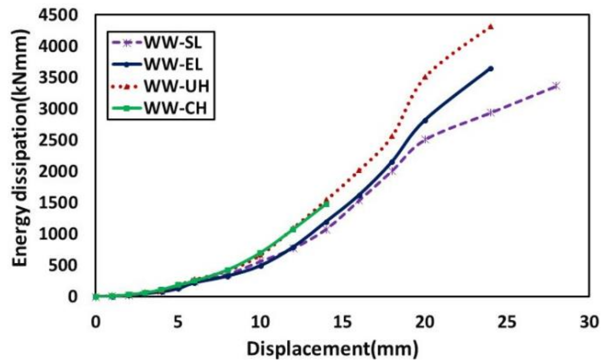

Fig. 23 Energy dissipation capacity of all the connections

11.5 Stiffness degradation

A stiffness degradation of a reinforced concrete structure describes the characteristic of crack formation, loss of bond between concrete and steel, and interaction with high shear or axial stresses. The stiffness degradation was calculated as the peak to peak load change of each displacement cycle. It was mainly dependent upon the material properties, geometry, level of ductile detailing, connection type, and the loading history of the structure (FEMA P440A 2009). The following Eq. (1) was used in the calculation of the stiffness degradation.

$$K_i = \frac{\{+Fi\}+\{-Fi\}}{\{+\Delta i\}+\{-\Delta i\}} \text{(Ni, } \textit{et.al.}\text{2019)} \qquad (1)$$

where,

$+F_i$ and $-F_i$=the positive and negative lateral peak loads of the i^{th} hysteretic loop.

$+\Delta_i$ and $-\Delta_i$=the positive and negative lateral top displacements of the i^{th} hysteretic loop.

Initially, the stiffness was 30 kN/mm, 25 kN/mm, 28 kN/mm, and 33 kN/mm for specimens (WW-SL), (WW-EL), (WW-UH), and (WW-CH) respectively. Fig. 21 shows the stiffness degradation of all the connections. The stiffness degradation of the connection can be explained in two stages. In the first stage, the stiffness degradation was initially faster up to the 3mm displacement cycle. In the second stage, the stiffness degradation was gradual and smooth. The stiffness degradation of the specimen (WW-CH) was steep when compared to all the other specimens. Each secant stiffness value of a specific specimen was normalized with respect to the secant stiffness measured at 5 mm displacement level for comparison between the connections. The normalized stiffness degradation of all the connections is shown in Fig. 22. The normalized stiffness degradation of specimens (WW-EL) and (WW-UH) gradually decreased when compared to the other connections. The loss of stiffness from the initial stiffness of the specimens was 90%, 81%, 82%, and 69% for (WW-SL), (WW-EL), (WW-UH), and (WW-CH) connections, respectively. The normalized stiffness curve for specimen (WW-CH) was steeper compared to other connections due to sudden loss in stiffness.

11.6 Energy dissipation curve

The energy dissipation capacity is the amount of energy dissipated throughout the structure without reducing the strength and stiffness in the inelastic range during loading and unloading conditions (FEMA P440A 2009). It is equal to the area of the enclosed hysteretic loop during positive and negative cycles. The energy dissipation capacity of (WW-UH) connection was 22%, 15%, and 66% greater than the (WW-SL), (WW-EL) and (WW-CH) connections, respectively. The energy dissipation capacity of specimen (WW-EL) was 8% greater than the (WW-SL) connection. The energy dissipation capacity of all the connections is shown in Fig. 23. All the connections except connection (WW-CH) showed a similar pattern of energy dissipation throughout the displacement cycle. After cracking, the pinching effect reduced the energy dissipation capacity of each displacement cycle. The energy dissipation of connection (WW-CH) was similar to that of (WW-UH)

Table 3 Ductility of the connections

Specimen	Ultimate displacement		Yield displacement		Displacement ductility factor μ		Average displacement ductility factor
	Positive	Negative	Positive	Negative	Positive	Negative	
WW-SL	17.5	17.5	5	6	3.50	2.92	3.21
WW-EL	13.00	19.50	4.50	7.50	2.89	2.60	2.74
WW-UH	23.00	19.5	6.25	6.75	3.68	2.89	3.28
WW-CH	10.00	13.00	3.50	5.00	2.86	2.60	2.73

connection up to failure. The connection (WW-CH) failed at the 14 mm displacement cycle whereas the (WW-UH) connection failed at the 24 mm displacement cycle.

11.7 Ductility

The ductility defines the inelastic deformation of the structure subjected to wind and seismic excitation. The structure should be designed with the ability to withstand all kind of loads without a reduction in the strength of the structure. Connections play an important role in resisting the external load. The ductility is here defined as the ratio of the ultimate displacement to the corresponding displacement at yielding. The ultimate displacement corresponding to the displacement at 85% of the peak load was calculated according to Park and Paulay (1975). The yield displacement was calculated from the tangent drawn to the 0.75 times of the ultimate load (Park 1988). The average displacement ductility value of all the precast connections is shown in Table 3. The ductility of the specimen (WW-UH) was 16% and 17% greater than the (WW-EL) connection and (WW-CH) connection, respectively. The residual load capacity of the specimen (WW-SL) decreased gradually after the ultimate load which is an indication of a ductile behaviour. The ductility of the (WW-EL) connection was 14.6% lesser than that of the (WW-SL) connection. This was because of less confinement of concrete due to more spacing between the overlapping loops in the (WW-EL) connection. In general, all the connections exhibited a good ductile behaviour.

11.8 Equivalent viscous damping

When structures are subjected to seismic and wind loads, by providing damping, the vibration of the structure can be controlled. Equivalent viscous damping describes the nonlinear behaviour of the hysteretic loop corresponding to energy dissipation and energy stored in the connection. The equivalent damping ratio indicates the ability to control the structural response due to vibration and was calculated by the following Eq. (2).

$$\xi = \frac{1}{2\pi}\frac{A}{F_o U_o} \quad \text{(Rodrigues } et\ al. \text{ 2017)} \tag{2}$$

A=Area of half loop.

F_o=Maximum force at each displacement.

U_o=Displacement at corresponding force.

The equivalent viscous damping ratio of the precast connections was calculated above 1% drift as shown in Fig. 24. Up to 1% drift all the precast connections behaved

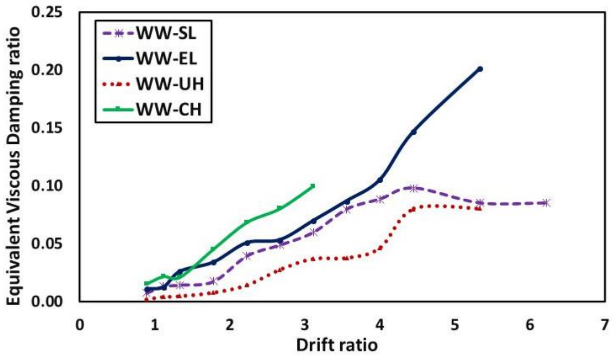

Fig. 24 Equivalent viscous damping ratio of all the connections

elastically. For all the precast connections up to 4% drift, equivalent viscous damping ratio increased linearly. Beyond 5% drift, the equivalent viscous damping ratio increased in specimen (WW-EL) and also viscous damping ratio was 60% and 58% greater than specimens (WW-UH) and (WW-SL), respectively. Specimen (WW-EL) had a higher energy absorption capacity in the elasto-plastic region, with respect to the energy stored in the elastic region, as compared to the other connections.

11.9 Crack pattern

Figs. 25-28 show the crack pattern of specimens (WW-SL), (WW-EL), (WW-UH), and (WW-CH), respectively. The first crack was formed at the 5 mm displacement cycle in the connections (WW-SL) and (WW-EL). In specimen (WW-SL) most of the cracks were formed at the interface. Inclined cracks were formed from the bottom of the left panel towards the connection. Cracks developed from the foundation and growing towards the inside the wall in both the connections. In the (WW-EL) connection, at the -14mm displacement cycle, spalling of concrete was seen at the right wall connection junction. Following this, the spalling of concrete was observed between the connection and the bottom left panel at the -16 mm displacement cycle. Finally, the reinforcement was exposed at the bottom of the connection region at the -24 mm displacement cycle, diagonal cracks and interface cracks were formed in both the connections. The displacement was applied till the 28 mm and 24 mm displacement cycles for (WW-SL) and (WW-EL) connections, respectively.

In specimen (WW-UH) an initial crack was formed at the 8 mm displacement cycle and the connection reinforcement was exposed in the bottom of the connection at the -18 mm displacement cycle. Then, a crack was initiated from the right wall panel and developed to the left wall panel through the connection. In specimen (WW-CH) an initial crack was formed at the -2 mm displacement cycle. A crack width of 5 mm was developed between the left wall panel and the connection at the -8 mm displacement cycle. A crack was measured between the top of the right wall panel and the connection with a 10 mm width at the -10 mm displacement cycle. Finally, the specimen (WW-CH) failed at the 12 mm displacement cycle with a sudden detachment of the channel section from

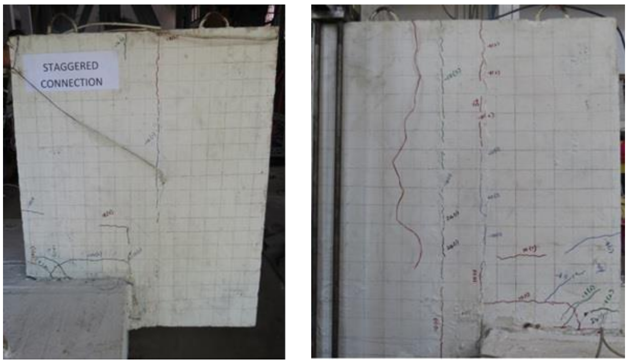

Fig. 25 Crack pattern for specimen (WW-SL) at 6.2% drift ratio (a) Front side (b) Back side

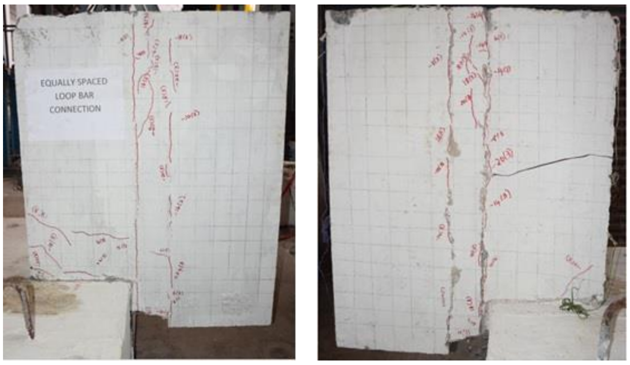

Fig. 26 Crack pattern for specimen (WW-EL) at 5.3% drift ratio (a) Front side (b) Back side

Fig. 27 Crack pattern for specimen (WW-UH) at 5.3% drift ratio (a) Front side (b) Back side

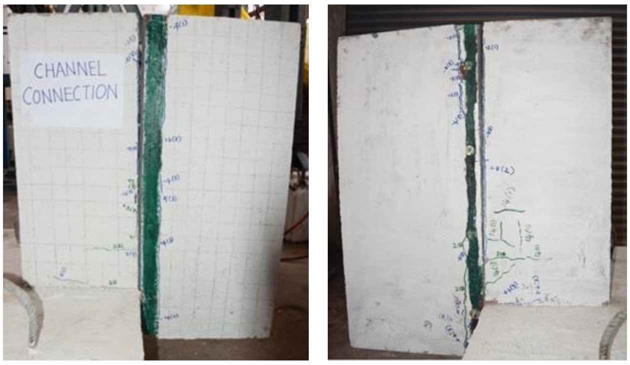

Fig. 28 Crack pattern for specimen (WW-CH) at 3.1% drift ratio (a) Front side (b) Back side

the wall panel. All the specimens showed a ductile failure mode as all the connections were able to sustain the load after the ultimate displacement.

12. Conclusions

This paper presents studies on the behaviour of wall to wall vertical connections subjected to reverse cyclic loading. Three wet connections in shape of, (i) Staggered Loop bar connection (WW-SL), (ii) Equally spaced Loop bar connection (WW-EL), (iii) U-Hook connection (WW-UH), and one dry connection named Channel connection (WW-CH) were considered for the experimental investigation. The summary of the observations are as follows.

- The ultimate load carrying capacity of all the four connections were almost equal in the positive direction (upward loading). But in the negative direction (downward loading), except channel connection (WW-CH), the remaining three connections exhibited a similar load carrying capacity. This may be due to the presence of the same area of shear reinforcement in all three specimens (WW-SL), (WW-EL), and (WW-UH). But in the channel connection the amount of shear reinforcement was less in the connection region compared to other connections.
- For the connection (WW-EL), though the spacing between the overlapping loops was adopted greater than 6ϕ, the load carrying capacity was 2.63% and 1.26% greater than that of (WW-SL) connection in the positive and negative direction, respectively.
- The (WW-EL) connection exhibited a 14.6% lesser ductility, when compared to the (WW-SL) connection. This was because the confinement of concrete in the connection region between the overlapping loops was less due to more spacing between the overlapping loops
- A sudden drop in load carrying capacity of specimen (WW-CH) was due to detachment of the channel section from the concrete panel.
- In all the wet connections, the hysteresis loops were wide and stable. In the case of the channel connection, the hysteresis loops were narrow. This indicates that the energy dissipation of the channel connection was less than the other three connections.
- Though, in terms of buildability, the channel section is easier to construct, considering its performance with respect to ultimate load carrying capacity, ductility, and energy dissipation, it is not favourable for the precast wall to wall vertical connection.
- As the confinement of the grout provided by the reinforcement in the connection region was effective, the load ratio was stable for a longer displacement range, even beyond the ultimate load for all the three wet connections.
- The specimen (WW-UH) exhibited greater energy dissipation capacity and ductility when compared to all the other connections.
- Considering various parameters like ultimate load carrying capacity, ductility, and energy dissipation, the

U-Hook connection (WW-UH) has shown better performance than the other three connections.

• Based on this observation, the authors recommend the U-Hook connection for the wall to wall vertical connection.

Acknowledgements

The Authors gratefully acknowledge the technical support rendered by the Structural Dynamics Laboratory at Anna University, Chennai.

References

Ajrab, J.J., Pekcan, G. and Mander, J.B. (2004), "Rocking wall-frame structures with supplemental tendon systems", *J. Struct. Eng.*, ASCE, **130**(6), 895-903. https://doi.org/10.1061/(ASCE)0733-9445(2004)130:6 (895).

Alameddine, F. and Ehsani, M.R. (1991), "High-strength RC connections subjected to inelastic cyclic loading", *J. Struct. Eng.*, ASCE, **117**(3), 829-850. https://doi.org/10.1061/(ASCE)0733-9455(1991)117:3 (829).

Araujo, D.L., Curado, M.C. and Rodrigues, P.F. (2014), "Loop connection with fibre reinforced precast concrete components in tension", *Eng. Struct.*, **72**, 140-151. https://doi.org/10.1016/j.engstruct.2014.04.032.

Belleri, A., Schoettler, M.J., Restrepo, J.I. and Fleischman, R.B. (2014), "Dynamic behaviour of rocking and hybrid cantilever walls in a precast concrete building", *ACI Struct. J.*, **111**(3), 661-671.

Biswal, A., Prasad, A.M. and Sengupta, A.K. (2018), "Study of shear behaviour of grouted vertical joints between precast concrete wall panels under direct shear loading", *Struct. Concrete*, **20**(2), 1-19. https://doi.org /10.1002/suco.201800064.

Cheok, G.S. and Lew, H.S. (1993), "Model precast concrete beam-to column connections subjected to cyclic loading", *PCI J.*, **38**(4), 80-92.

Erkmen, B. and Schultz, A.E. (2009), "Self-centering behavior of unbonded, post-tensioned precast concrete shear walls", *J. Earthq. Eng.*, **13**(7), 1047-1064. https://doi.org /10.1080/13632460902859136.

FEMA P440A (2009), Effects of Strength and Stiffness Degradation on Seismic Response, Applied Technology Council, California.

Henry, R.S., Brooke, N.J., Sritharan, S. and Ingham, J.M. (2012), "Defining concrete compressive strain in unbonded post-tensioned walls", *ACI Struct. J.*, **109**(1), 101-111.

Hofheins, C.L., Reaveley, L.D. and Pantelides, C.P. (2002), "Behavior of welded plate connections in precast concrete panels under simulated seismic loads", *PCI J.*, **47**(4), 122-133. https://doi.org/10.15554/pcij. 07012002.122.133.

Holden, T., Restrepo, J. and Mander, J.B. (2003), "Seismic performance of precast reinforced and prestressed concrete walls", *J. Struct. Eng.*, ASCE, **129**(3), 286-296. https://doi.org/10.1061/(ASCE)0733-9445(2003)129:3(286).

Ibrahim, I.S., Padil, K.H., Bady, H.M.A., Saim, A.A. and Sarbini, N.N. (2014), "Ultimate shear capacity and failure of shear key connection in precast concrete construction", *Malays. J. Civil Eng.*, **26**(3), 414-430.

IS 10262 (2009), Guidelines for Concrete Mix Design Proportioning, Bureau of Indian Standard, New Delhi.

IS 13920 (2016), Code of Practice for Ductile Detailing of Reinforced Concrete Structures Subjected to Seismic Forces, New Delhi.

IS 456 (2000), Indian Standard Code of Practice for Plain and Reinforced Concrete, New Delhi.

IS 800 (2007), Code of Practice for General Construction in Steel, New Delhi.

Joergensen, H.B. and Hoang, L.C. (2013), "Tests and limit analysis of loop connections between precast concrete elements loaded in tension", *Eng. Struct.*, **52**, 558-569. https://doi.org/10.1016/j.engstruct. 2013.03.015.

Joergensen, H.B. and Hoang, L.C. (2015), "Load carrying capacity of keyed joints reinforced with high strength wire rope loops", *Proceedings of fib Symposium 2015*.

Joergensen, H.B., Hoang, L.C. and Hagsten, L.G. (2017), "Strength of precast concrete shear joints reinforced with high-strength wire ropes", *Inst. Civil Eng. Proc. Struct. Build.*, **170**(3), 168-179. https://doi.org/10.1680/jstbu.16.00096.

Kam, W.Y., Pampanin, S. and Elwood, K. (2011), "Seismic performance of reinforced concrete buildings in the 22 February Christchurch (Lyttelton) earthquake", *Bull. N.Z. Soc. Earthq. Eng.*, **44**(4), 239-278. https://doi.org/10.5459/bnzsee.44.4.239-278.

Kurama, Y.C. (2005), "Seismic design of partially post-tensioned precast concrete walls", *PCI J.*, **50**(4), 100-125.

Li, L. and Jiang, Z. (2016), "Flexural behavior and strut and tie model of joints with headed bar details connecting precast members", *Perspect. Sci.*, **7**, 253-260. https://doi.org/10.1016/j.pisc.2015. 11.041.

Marriott, D., Pampanin, S., Bull, D.K. and Palermo, A. (2008), "Dynamic testing of precast, post-tensioned rocking wall systems with alternative dissipating solutions", *Bull. N.Z. Soc. Earthq. Eng.*, **41**(2), 90-103. https://doi.org/10.5459/bnzsee.41.2.90-103.

Ni, X., Cao, S., Li, Y. and Liang, S. (2019), "Stiffness degradation of shear walls under cyclic loading: experimental study and modelling", *B. Earthq. Eng.*, **17**(9), 5183-5216. https://doi.org/ 10.1007/s10518-019-00682-5.

Ong, K.C.G., Hao, J.B. and Paramasivam, P. (2006), "Flexural behavior of precast joints with horizontal loop connections", *ACI Struct. J.*, **103**(5), 664-671.

Park, R. (1988), "State-of-the art report on ductility evaluation from laboratory and analytical testing", *Proceedings of the 9th World Conference on Earthquake Engineering*, Science Council of Japan, Tokyo.

Park, R. (2003), "The fib state-of-the-art report on the seismic design of precast concrete building structures", *Pacific Conference on Earthquake Engineering*.

Park, R. and Paulay, T. (1975), *Reinforced Concrete Structures*, Wiley, New York.

Perez, F.J., Pessiki, S. and Sause, R. (2013), "Experimental lateral load response of unbonded post-tensioned precast concrete walls", *ACI Struct. J.*, **110**(6), 1045-1055.

Perez, F.J., Sause, R. and Pessiki, S. (2007), "Analytical and experimental lateral load behavior of unbonded post tensioned precast concrete walls", *J. Struct. Eng.*, ASCE, **133**(11), 1531-1540. https://doi.org/10.1061/(ASCE)0733-9445(2007) 133:11(1531).

Pramodh, R., Shripriyadharshini, V. and Vidjeapriya, R. (2018), "Shear behavior of horizontal joints between precast panels", *Asian J. Civil Eng.*, **19**(1), 651-662. https://doi.org/10.1007/s42107-018-0053-0.

Restrepo, J.I. and Rahman, A. (2007), "Seismic performance of self centering structural walls incorporating energy dissipators", *J. Struct. Eng.*, ASCE, **133**(11), 1560-1570. https://doi.org/10.1061/(ASCE)0733-9445(2007)133:11(1560).

Rodrigues, H., Furtado, A. and Arede, A. (2017), "Experimental evaluation of energy dissipation and viscous damping of repaired and strengthened RC columns with CFRP jacketing under biaxial load", *Eng. Struct.*, **145**, 162-175.

https://doi.org/10.1016/j.engstruct.2017.05.021.

Rossley, N., Aziz, F.N.A.A. and Chew, H.C. (2014a), "Behaviour of precast walls connection subjected to shear load", *J. Eng. Sci. Technol*., **10**, 142-150.

Rossley, N., Aziz, F.N.A.A., Chew, H.C. and Farzadnia, N. (2014b), "Behaviour of vertical loop bar connection in precast wall subjected to shear load", *Aust. J. Basic Appl. Sci*., **8**(1), 370-380.

Ryu, H.K., Kim, Y.J. and Chang, S.P. (2007), "Experimental study on static and fatigue strength of loop joints", *Eng. Struct*., **29**(2), 145-162. https://doi.org/10.1016/j.engstruct.2006.04.014.

Shen, S.D., Pan, P., Miao, Q.S., Li, W.F. and Gong, R.H. (2019), "Behaviour of wall segments and floor slabs in precast reinforced concrete shear walls assembled using steel shear keys", *Struct. Control Hlth*., **301**(15), 13-19. https://doi.org/10.1002/stc.2418.

Smith, B.J. and Kurama, Y.C. (2014), "Seismic design guidelines for solid and perforated hybrid precast concrete shear walls", *PCI J*., **59**(3), 43-59. https://doi.org/ 10.15554/pcij.06012014.43.59.

Smith, B.J., Kurama, Y.C. and McGinnis, M.J. (2011), "Design and measured behavior of a hybrid precast concrete wall specimen for seismic regions", *J. Struct. Eng*., **137**(10), 1052-1062. https://doi.org/ 10.1061/(ASCE)ST.1943-541X.0000327.

Smith, B.J., Kurama, Y.C. and McGinnis, M.J. (2013), "Behavior of precast concrete shear walls for seismic regions: Comparison of hybrid and emulative specimens", *J. Struct*. *Eng*., **139**(11), 1917-1927. https://doi.org/10.1061/(ASCE)ST.1943-541X.0000755.

Smith, B.J., Kurama, Y.C. and McGinnis, M.J. (2015), "Perforated hybrid precast shear walls for seismic regions", *ACI Struct. J*., **112**(3), 359-370. https://doi.org/10.14359/51687410.

Smith, D.J.P. (2016), "Investigation of grouted dowel connection for precast concrete wall construction", Electronic Thesis and Dissertation Repository, 4298.

Sorensen, J.H., Herfelt, M.A., Hoang, L.C. and Muttoni, A. (2018), "Test and lower bound modeling of keyed shear connection in RC shear walls", *Eng. Struct*., **155**, 115-126. https://doi.org/ 10.1016/j.engstruct. 2017.11.004.

Sorensen, J.H., Hoang, L.C., Fischer, G. and Olesen, J.F. (2015), "Construction-friendly ductile shear joints for precast concrete panels", *Proceedings of the International Conference on Performance-based and Life-cycle Structural Engineering*.

Sorensen, J.H., Hoang, L.C., Olesen, J.F. and Fischer, G. (2016), "Test and analysis of a new ductile shear connection design for RC shear walls", *Struct. Concrete*, **18**(1), 189-204. https://doi.org/10.1002/suco. 201600056.

Sorensen, J.H., Hoang, L.C., Olesen, J.F. and Fischer, G. (2017a), "Testing and modeling dowel and catenary action in rebars crossing shear joints in RC", *Eng. Struct*., **145**, 234-245. https://doi.org/10.1016/j. engstruct.2017.05.020.

Sorensen, J.H., Hoang, L.C., Olesen, J.F. and Fischer, G. (2017b), "Tensile capacity of loop connections grouted with concrete or mortar", *Mag. Concrete Res*., **69**(17), 892-904. https://doi.org/ 10.1680/ jmacr.16.00466.

Soudki, K.A., West, J.S., Rizkalla, S.H. and Blackett, B. (1996), "Horizontal connections for precast concrete shear wall panels under cyclic shear loading", *PCI J*., **41**(3), 64-80.

Taheri, H., Hejazi, F., Vaghei, R., Jaafar M.S. and Ali, A.A.A. (2016), "New precast wall connection subjected to rotational loading", *Period. Polytech-Civil*, **60**(4), 547-560. https://doi.org/10.3311/PPci.8545.

Vaghei, R., Hejazi, F., Taheri, H., Jaafar, M.S. and Ali, A.A.A. (2016), "A new precast wall connection subjected to monotonic loading", *Comput. Concrete*, **17**(1), 1-27. https://doi.org/10.12989/cac. 2016.17.1.001.

Vaghei, R., Hejazi, F., Taheri, H., Jaafar, M.S. and Aziz, F.N.A.A. (2017), "Development of a new connection for precast concrete walls subjected to cyclic loading", *Earthq. Eng. Eng. Vib*., **16**(1), 97-117. https://doi.org/ 10.1007/s11803-017-0371-3.

Vaghei, R., Hejazi., F., Firoozi, A.A. and Jaafar M.S. (2019), "Performance of loop connection in precast concrete walls subjected to lateral loads", *Int. J. Civil Eng*., **17**(3), 397-426. https://doi.org/10.1007/ s40999-018-0366-0.

Vidjeapriya, R. and Jaya, K.P. (2013), "Experimental study on two simple mechanical precast beam-column connections under reverse cyclic loading", *J. Perform. Constr. Facil*., ASCE, **27**(4), 402-414. https://doi.org/10.1061/(ASCE)CF.1943-5509.0000324.

Yu, H.J., Kang, S.M., Park, H.G. and Chung, L. (2019), "Cyclic loading test of structural walls with small openings", *Int. J. Concrete Struct. Mater*., **13**(1), 40. https://doi.org/10.1186/s40069-019-0352-1.

JK